MODELING AND CONTROL OF THERMAL MICROSYSTEMS

Yong Joon Lee*, Su Whan Sung, Dae Sung Yoon***, Geunbae Lim***, and Sunwon Park***

**Department of Chemical & Biomolecular Engineering and Center for Ultramicrochemical Process Systems, Korea Advanced Institute of Science and Technology*
373-1, Gusung-dong, Yusung-gu, Daejon, 305-701, KOREA

***Corporate R&D, LG Chem. Ltd. Research Park*
104-1, Moonji-dong, Yusung-gu, Daejon, 305-380, KOREA

****Biochip Project Team and MEMS Lab., Samsung Advanced Institute of Technology*
San 14 Nongseo-Ri, Kiheung-Eup, Yongin-City, Kyunggi-Do, 449-712, KOREA

Abstract: A thermal microsystem is developed which consists of a microreactor integrated with a platinum sensor/heater, and automation equipment/software such as data acquisition system, control program and graphic user interface. From the control point of view, we analyze the dynamic characteristics of the fabricated microreactor and find some interesting dynamic features. On the basis of the analysis, we suggest an appropriate model structure and estimate the model parameters using the prediction error identification method. Requirements for a high-performance operation are discussed and a nonlinear control strategy is proposed to linearize the nonlinear dynamics of the thermal microsystem. We determine the parameters of the nonlinear controller using the optimal tuning method. The developed thermal microsystem shows much better control performances compared to commercial polymerase chain reaction (PCR) thermal cyclers. We successfully demonstrate the PCR of plasmid DNA using the thermal microsystem.

Keywords: Thermal Microsystems, System Identification, Nonlinear Control, PID Controller , Polymerase Chain Reaction

1. INTRODUCTION

The miniaturized processes integrated with microreactors, microsensors and microactuators using semiconductor fabrication technologies can realize extremely high efficiency and high throughput operation as well as surprising reduction of reagents, cost, reaction time, power etc. The thermal microsystem is one of the most typical miniaturized processes. In particular, it is useful for DNA polymerase chain reaction (PCR) that requires rapid temperature control to shorten the total running time and precise temperature control for high efficiency. Many types of thermal microsystems have been proposed. Belgrader et al. (2001) developed a compact, battery-powered fluorometric thermal cycler that consisted of two reaction modules for multiplex real-time PCR. Northrup et al. (1988) designed a portable thermal cycle system including silicon-based reaction chambers with integrated heaters for efficient temperature control and optical windows for real-time fluorescence monitoring. Lao et al. (2000) fabricated a silicon-based thermal microsystem and demonstrate its precise temperature control, rapid heating and cooling. They used a gain-scheduling algorithm for the proportional-integral (PI) controller to incorporate the nonlinearity of the thermal cycler.

In this research, we mainly focus on a systematic modeling and control of the thermal microsystem in the hope that the system level analysis and optimization would contribute to maximizing the performance of the thermal microsystem and provide some insights on the optimal operation. We fabricate a silicon-based microreactor integrated with a platinum sensor/heater and hardware/software for

data acquisition, control and power supply. The dynamic thermal characteristics of the thermal microsystem is analyzed especially, from the control and modeling point of view. We propose an appropriate model structure on the basis of the dynamics analysis and estimate the model parameters using the prediction error identification method. Requirements for the high performance operation are discussed and a nonlinear control strategy linearizing the nonlinear dynamics of the thermal microsystem is proposed. We use the optimal tuning method to obtain the adjustable parameters of the controller.

2. THERMAL MICROSYSTEM

We manufactured the thermal microsystem as shown in Figure 1a. It is composed of six parts: silicon-based microreactor, cooling fan, amplification circuit, data acquisition, external power supplier, software for the automatic control algorithm and graphic user interface. The control signal of the thermal microsystem flows like the following: The amplification circuit amplifies the voltage of the platinum sensor (equivalently, the temperature of the microreactor) and transfers the amplified voltage to the analog input of the data acquisition system as shown in Figure 1a. Then, the automatic control algorithm adjusts the analog output to control the temperature as fast and precisely as possible and the graphic user interface graphically displays the temperature and the analog output on screen. Subsequently, the external power supplier powers the platinum heater in proportion to the analog output of the data acquisition system. Then, the voltage of the platinum sensor (equivalently, the temperature of the microreactor) changes and passes through the amplification circuit again. The whole procedure is repeated every sampling time.

The amplification circuit plays an important role in increasing the resolution in reading the temperature. The platinum heater connected to the external power supplier is to heat the microreactor while the cooling fan is for rapid cooling of the microreactor. We use a nonlinear proportional-integral (PI) controller as the control algorithm. The graphic user interface is a useful tool for users who are unfamiliar with the system to operate the thermal microsystem as he/she wants. The graphical user interface includes various functions for user's conveniences such as easy real-time scheduling of the desired temperature profile, manual setting of the controller tuning parameters, real-time plotting of the temperature and so on.

The silicon-based microreactor was integrated with thin-film platinum sensor and heater. The microchip in Figure 1b is fabricated through several steps as shown in Figure 2. At step 4, the silicon is etched to 100 μ m depth with tetramethylammoniumhydroxide (TMAH) for the microreactor and the microchannel. The thermal oxide film at step 5 serves as an electrical insulation layer. At step 7, titanium (Ti) film and platinum (Pt) film are deposited by dc off-axis magnetron sputtering.

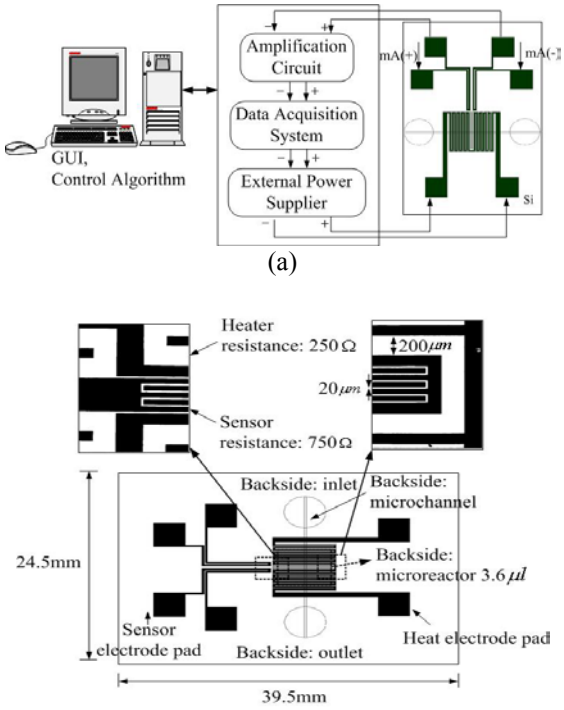

Fig. 1. Thermal Microsystems: (a) Overall scheme, (b) Top view of the microreactor

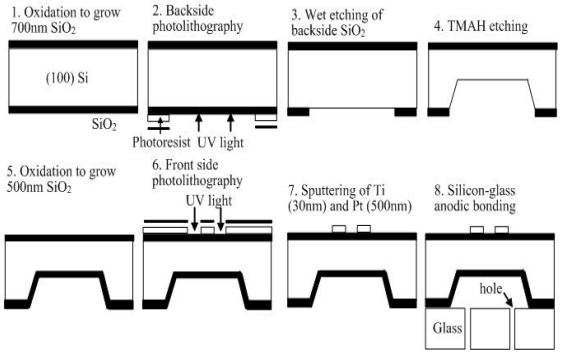

Fig. 2. Fabrication steps of the microreactor

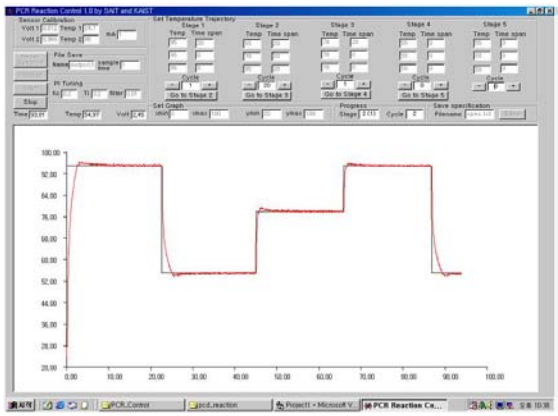

Fig. 3. Graphic user interface

To guarantee a high resolution in the data acquisition, the following devices are integrated for the data acquisition system: the AD7715 of Analog Devices, Inc. for the 16bit analog input, the DAC8043 of Analog Devices, Inc. for the 12bit analog output and the AT89C2051 microcontroller of ATMEL, Inc. to communicate with the personal computer.

3. MODELING OF THERMAL MICROSYSTEM

In this section, we develop a model to mathematically represent the dynamics between the reactor temperature and the voltage applied to the heater.

3.1 Determining Model Structure

Before we estimate the model parameters, we should determine the model structure. The following five items are considered for the best model structure selection.

1) For electrical heating systems like thermal microsystems, the voltage has been frequently chosen as the input of the model. However, the choice is not good because the temperature is in proportion to the electrical power rather than the voltage. Consider the following relationship between the power and the voltage.

$$p = \frac{v^2}{R} \tag{1}$$

where, p and v represent the power and the voltage. R denotes the resistance of the heater. If we choose the voltage as the model input, the square nonlinearity between the model output (temperature) and the model input (voltage) cannot be avoided. The nonlinearity makes the controller design complicated and seriously degrades the control performance. So, we should choose the square of the voltage (v^2) as the model input to avoid the nonlinearity.

2) A step test is one of the simplest techniques to detect the dynamic characteristics of the process. Figure 3 shows the step response of the thermal microsystem. It should be noted that there is a sudden jump from the initial temperature (67.9 ^{o}C) up to around 80 ^{o}C at the instance of the input change. This is strong evidence that the transfer function from the input (i.e., the square of the voltage) to the output (i.e., the temperature) includes a small negative 'zero' (here, 'zero' is defined as the solution that makes the transfer function zero). For a simple justification for the statement, consider the following second order transfer function for example.

$$y(s) = \frac{5s+1}{4s^2+10s+1}u(s) \tag{2}$$

Where $u(s)$ and $y(s)$ are the Laplace transform of the input and the output, respectively.

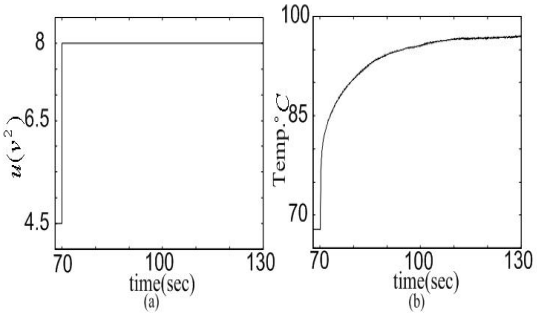

Fig. 4. Step response of the thermal microsystem: (a) step input, (b) temperature

The transfer function has a negative zero of –0.2. To understand the effect of the negative 'zero', rewrite (2) as follows.

$$y_1(s) = \frac{5s}{4s^2+10s+1}u(s) \tag{3}$$

$$y_2(s) = \frac{1}{4s^2+10s+1}u(s) \tag{4}$$

$$y(s) = y_1(s) + y_2(s) \tag{5}$$

where $y_1(s)$ corresponds to the effect of the negative 'zero' on the process output $y(s)$ that includes the time-derivative of the input (i.e., $5su(s)$, equivalently, $5du(t)/dt$).

The time-derivative ($du(t)/dt$) of the input jumps from zero to infinite at the instance of the step input change and again becomes zero after the instance. But, such a sudden jump cannot be expected from the transfer function of (4) because it does not include the derivative term of the input. Putting it all together, we can realize that the initial jump comes from the small negative 'zero'.

3) We also recognize from the step response of Figure 4 that there is nearly no time delay between the input and the output. The existence of time delays seriously deteriorates the maximum achievable control performance of the feedback control system. The observation of nearly zero time delay is very favourable for us to design a high performance feedback controller.

4) Another dynamic characteristic of the step response is that the jump is not a vertical line and the transition from the initial jump to the next dynamic response of the temperature is smooth rather than clearly separated. This means that the order of the dynamic system is at least two. Let us consider the dynamics of the first order dynamic system as follows:

$$y(s) = \frac{k_2 s + k_1}{\tau s + 1}u(s) = \frac{k_2}{\tau}u(s) + \frac{k_1 - k_2/\tau}{\tau s + 1}u(s) \tag{6}$$

From inspecting (6), we recognize that the step response $y(s)$ is a combination of the static value of $(k_2/\tau)u(s)$ and the dynamic response of $(k_1 - k_2/\tau)u(s)/(\tau s + 1)$. Therefore, the jump should be totally vertical line and the transition should be clearly separated if the process is the first order system with a 'zero'. This implies that the process order is at least two.

5) Finally, it should be noted that there is always a small input nonlinearity due to various causes like the resistance variation of the heater during heating, nonlinear characteristic of the data acquisition system and the power supplier etc.

Putting it all together, we should consider the following requirements to choose an appropriate model structure for the thermal microsystem:

1. The input and output of the dynamic model should be the square of the voltage and the microreactor temperature, respectively.
2. The dynamic model should contain a small negative 'zero'.
3. The time delay can be chosen as zero.
4. The order of the dynamic thermal microsystem is at least two.
5. Input nonlinearity should be included.

Especially, if the model does not satisfy the first and second requirement, we cannot achieve acceptable model performances in a way of increasing the number of the model parameters.

We suggest the following nonlinear model structure that satisfies the above model requirements.

$$u(t) = v(t)^2 \tag{7}$$

$$q(t) = u(t) + p_1 u^2(t) + \cdots + p_{m-1} u^m(t) \tag{8}$$

$$\frac{dx(t)}{dt} = Ax(t) + Bq(t) \tag{9}$$

$$y(t) = Cx(t) + e(t) \tag{10}$$

Where $u(t)$ and $y(t)$ denote the model input (the square of the voltage) and the model output (the temperature), respectively. $e(t)$ is a white measurement noise. $x(t)$ is the n-dimensional state. System matrices A and B have the following respective forms:

$$A = \begin{bmatrix} 0 & 0 & 0 & \cdots & 0 & -a_n \\ 1 & 0 & 0 & \cdots & 0 & -a_{n-1} \\ 0 & 1 & 0 & \cdots & 0 & -a_{n-2} \\ \vdots & \vdots & \vdots & \vdots & \vdots & \vdots \\ 0 & 0 & 0 & \cdots & 0 & -a_2 \\ 0 & 0 & 0 & \cdots & 1 & -a_1 \end{bmatrix} \tag{11}$$

$$B = \begin{bmatrix} b_n & b_{n-1} & b_{n-2} & \cdots & b_2 & b_1 \end{bmatrix}^T \tag{12}$$

$$C = \begin{bmatrix} 0 & 0 & 0 & \cdots & 0 & 1 \end{bmatrix} \tag{13}$$

Here, (8) is the nonlinear static function and the system of (9) and (10) is the linear dynamic system. For readers who are familiar with time series expression, (9) and (10) can be rewritten equivalently like the following continuous-time output error (OE) model:

$$\begin{aligned} &z^{(n)}(t) + a_1 z^{(n-1)}(t) + \cdots + a_{n-1} z^{(1)}(t) + a_n z(t) \\ &= b_1 q^{(n-1)}(t) + b_2 q^{(n-2)}(t) + \cdots + b_{n-1} q^{(1)}(t) + b_n q(t) \end{aligned} \tag{14}$$

$$y(t) = z(t) + e(t) \tag{15}$$

where $z^{(i)}(t)$ denotes the i-th derivative of the continuous-time signal $z(t)$.

The chosen dynamic model of (7)-(15) satisfies the model requirements as follows: (7) is to satisfy the first requirement. If we do not fix $b_i, i = 1,2,\cdots,n-1$ at zeros, the second requirement would be satisfied. Because (9) does not include time delay, the third requirement is satisfied. The process order of the dynamic system composed of (9) and (10) is n. So, it should be $n \geq 2$ to satisfy the fourth requirement. The fifth requirement is incorporated by the nonlinear equation of (8).

3.2 Estimating Model Parameters

The simple first or second order plus time delay model (here, 'simple' means that the transfer function has no 'zero') has been widely used in industry to describe the process dynamics and to tune the proportional-integral-derivative (PID) controller (Seborg et al., 1989). However, the dynamic behavior of the thermal microsystem is far from the simple first or second order dynamic system because it contains a small negative 'zero'. So, we cannot use previous process reaction curve identification method, which is to identify only simple transfer functions. In this research, we use the prediction error identification method (Sung et al., 2001). It estimates the model parameters by minimizing the cost function as follows.

$$\min_{\hat{P},\hat{A},\hat{B}} \left[V(\hat{P},\hat{A},\hat{B}) = \frac{0.5}{N} \sum_{i=1}^{N} (y(t_i) - \hat{y}(t_i))^2 \right] \tag{16}$$

subject to

$$u(t) = v^2(t) \tag{17}$$

$$\hat{q}(t) = u(t) + \hat{p}_1 u^2(t) + \cdots + \hat{p}_{m-1} u^m(t) \tag{18}$$

$$\frac{d\hat{x}(t)}{dt} = \hat{A}\hat{x}(t) + \hat{B}\hat{q}(t) \tag{19}$$

$$\hat{y}(t) = C\hat{x}(t) \tag{20}$$

$$t_0 = 0 < t_1 < \cdots < t_{N-1} < t_N \tag{21}$$

where, $y(t)$ and $\hat{y}(t)$ denote the measured process output and the predicted model output, respectively. (17)-(20) are the optimal predictor for the process of (7)-(10). To solve the optimization problem, we use the Levenberg-Marquardt optimization method because its convergence rate is fast and robust. All equations to calculate the derivatives of the cost function in the Levenberg-Marquardt method can be easily derived from (16)-(20) as done in Sung et al. (2001).

3.3 Model Performances

We activated the thermal microsystem using roughly tuned PI controller to generate the test data. Table 1 shows the model performances of three linear model types: (1) the simple linear second order model with $v^2(t)$ as the model input ($n = 2$, $b_1 = 0$, $u(t) = v^2(t)$,

$m=1$); (2) the linear second order model which has a 'zero' and the voltage as the model input ($n=2, u(t)=v(t), m=1$); (3) the linear second order model which has a 'zero' and $v^2(t)$ as the model input ($n=2, u(t)=v^2(t), m=1$), respectively.

The simple linear second order model cannot well describe the dynamics because the model has no 'zero' as shown in Figure 5.

The model performance is inevitably poor due to the nonlinearity of the square function if the voltage is chosen as the model input as shown in Figure 6. The linear second order model which has a negative 'zero' and the square of the voltage as the model input can describe the dynamics more precisely than cases of Figure 6. Considering the remaining fifth model requirement, we can improve the model performance further by introducing the nonlinear polynomial to incorporate the nonlinear dynamics as shown in Figures 7 and 8. Table 1 shows the model performance of the second order model with the second order nonlinear polynomial function ($n=2$, $u(t)=v^2(t)$, $m=2$) and the third order nonlinear polynomial function ($n=2$, $u(t)=v^2(t), m=3$), respectively. Both show satisfactory identification results. We identified the third order dynamic model also. Its performance is almost the same as that of the second order model. We finally choose the model 4 of which the performance is shown in Figure 7 because it is simple while its performance is close to the best.

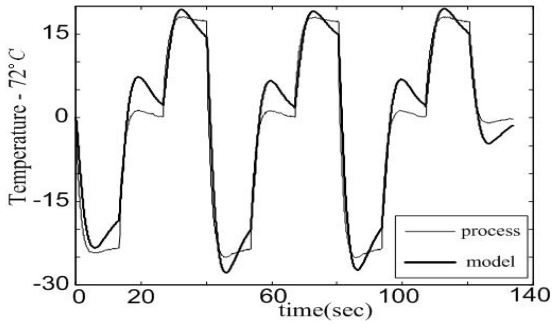

Fig. 5. Model performance when the model has no negative zero.

Table 1. Estimated model parameters and the modeling error (ISE-integral of the square error)

Model		Model parameters						ISE
No.	Structure	a_1	a_2	b_1	b_2	p_1	p_2	
1	$n=2, b_1=0$ $u(t)=v^2(t), m=1$	177.4			84.98			1232.4
2	$n=2$ $u(t)=v(t), m=1$	5.974	1.028	56.70	27.92			1464.5
3	$n=2$ $u(t)=v^2(t), m=1$	2.246	0.195	9.090	1.666			122.7
4	$n=2$ $u(t)=v^2(t), m=2$	2.657	0.281	9.781	2.236	0.0129		18.43
5	$n=2$ $u(t)=v^2(t), m=3$	2.604	0.272	9.790	2.194	0.0142	0.0010	17.84

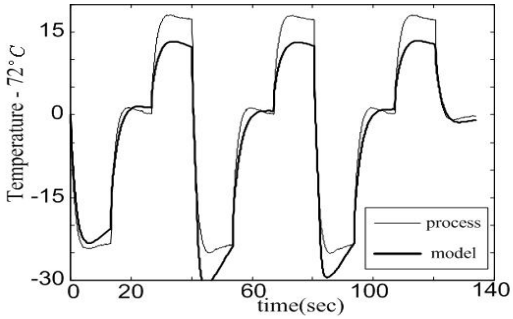

Fig. 6. Model performances when the input is voltage.

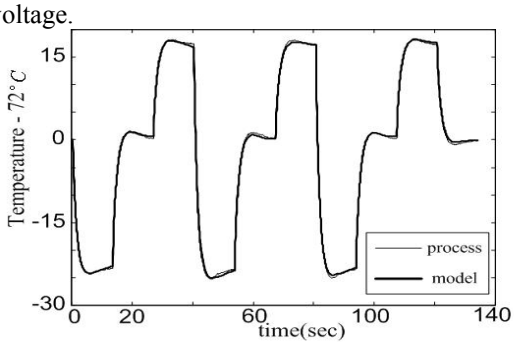

Fig. 7. Model performances when the model has a second order nonlinear polynomial.

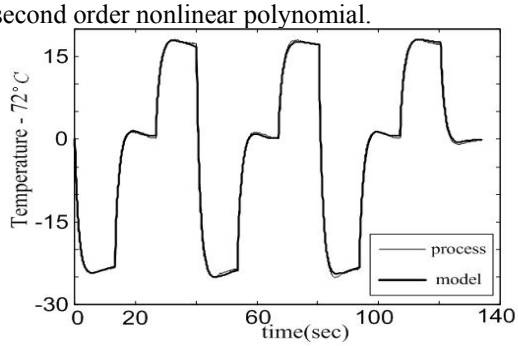

Fig. 8. Model performances when the model has a third order nonlinear polynomial.

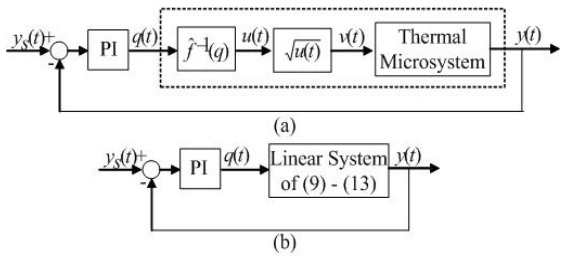

Fig. 9. Linearizing the nonlinear dynamics of the thermal microsystem: (a) The proposed nonlinear control strategy, (b) Equivalent control system

4. CONTROL STRATEGY

In this section, we will establish an automatic control strategy using the nonlinear proportional-integral (PI) controller as shown in Figure 9 on the basis of the identified nonlinear model. It satisfies the following three control requirements for high performance thermal microsystem.

4.1 Linearization

It should be noted that because the PI controller is a linear one, the corresponding process also should be linear to achieve the full performance of the PI controller. To satisfy the requirement, the proposed

control strategy linearizes the nonlinear dynamics of the thermal microsystem using the identified nonlinear model as shown in Figure 9a, where the dotted-line-box is equivalent to the linear process of (9)-(10) if the model is perfect. That is, the linear PI controller controls the linear process as shown in Figure 9b, which makes the tuning of the PI controller easier as well as guarantees high performances as in the linear case.

4.2 Tuning of the PI Controller

For the tuning of the proposed controller in Figure 9a, we don't have to consider the nonlinear parts of (17) and (18) because Figure 9a is essentially equivalent to Figure 9b. Then, we can tune the PI controller for the linear model of (19)-(20). To tune the PI controller, we estimate the tuning parameters by minimizing the following integral of the time-weighted square value of the error (ITSE) for the unit step set point change (Sung et al. (2002)).

$$\min_{k_p,k_i}\left\{V(k_p,k_i)=\sum_{i=1}^{N} t_i\left(y_d(t_i)-\hat{y}(t_i)\right)^2\Delta t\right\} \qquad (22)$$

subject to

$$\hat{q}(t)=k_p\left(y_s(t)-\hat{y}(t)\right)+k_i\sum_{i=1}^{N}\left(y_s(t_i)-\hat{y}(t_i)\right)\Delta t, \qquad (23)$$

$y_s(t)=1$

and (19)-(20)

where, k_p, k_i and Δt represent the proportional gain, integral gain and the sampling time. $y_s(t)$ and $\hat{y}(t)$ are the set point and the predicted model output, respectively. (23) is a mathematical representation of the PI controller. $y_d(t)$ denotes the user-specified desired trajectory which has the following form.

$$y_d(s)=\left(\frac{1}{\tau^2 s+1.414\tau s+1}\right)y_s(s) \qquad (24)$$

As we decrease the time constant τ, the closed-loop response becomes faster but more sensitive to the modeling error and shows a bigger overshoot. To solve the optimization problem, we use the Levenberg-Marquardt optimization method. For details, refer to Sung et al. (2002).

4.3 Integral Windup

The maximum achievable control performance for the thermal microsystem is very high because it has almost negligible time delay and no unstable 'zero's (Morari and Zafiriou, 1983). This means that we can raise the temperature up to the desired temperature within very short time only if we can afford to apply high voltage. But, we cannot increase the maximum voltage as high as we want because of the limited resolution of the data acquisition system (note that the resolution decreases as the maximum voltage increases) and cost problems. Then, the control output may be initially saturated at the maximum value for a large set point change (for example, from room temperature to 95 °C). The same situation happens in the cooling process. We should initially enter the minimum control output (i.e., zero voltage) for a while to drop the temperature as fast as possible. It is clear from the above argument that there should be inevitably actuator saturation for high performance operation. Then, the integral part of the PI controller accumulates too much when the control output is saturated, resulting in a large overshoot in the heating process and a large undershoot in the cooling process (Seborg et al., 1989). The situation is called "integral windup". In this research, when the control output is saturated, we stop the integral action of the PI controller to prevent the integral windup phenomenon.

4.4 Control Results

We choose $\tau = 0.2$ sec as the time constant of the desired trajectory and the sampling time is $\Delta t = 0.055$ sec. The estimated optimal tuning results for the desired trajectory are $k_c = 0.2107$ and $k_i = 0.2107/0.2242$.

We use the anti-windup technique. The control performance is excellent as shown in Figure 10. It shows remarkable heating and cooling rates of approximately 36 °C/sec and –22 °C/sec, about 15 times faster than commercial PCR machines.

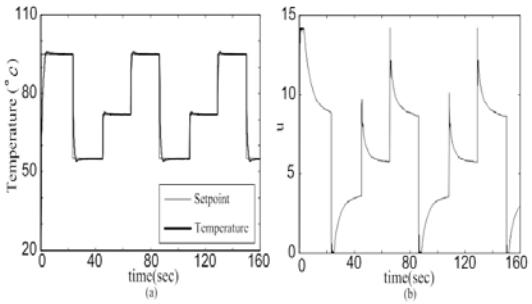

Fig. 10. Control performances of the proposed control strategy

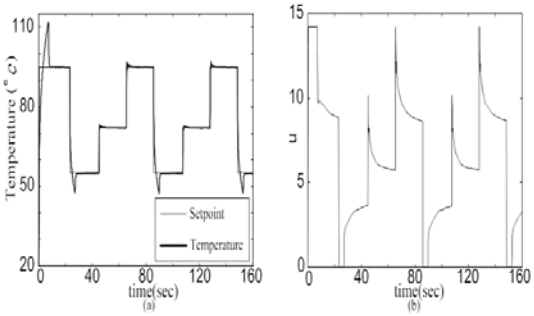

Fig. 11. Control performances of the nonlinear control strategy without anti-windup technique

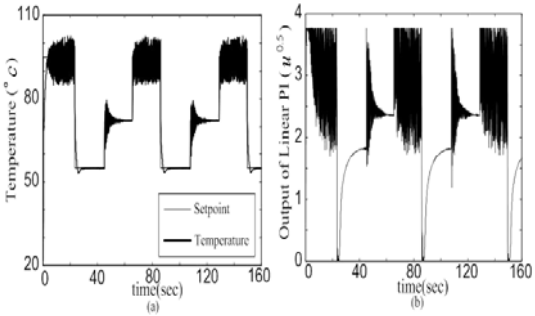

Fig. 12. Control performances of the linear PI controller

The overshoot was not over 0.8 ^{o}C and the steady state error is less than ±0.1 ^{o}C. Figure 11 shows what happen if we don't use anti-windup techniques.
There are a big overshoot and a big undershoot because the integral part of the PI controller becomes too big when the control output is saturated. We strongly recommend using the anti-windup function for the high-performance thermal microsystem. Figure 12 demonstrates what happen if we use only the linear PI controller without linearizing the nonlinear dynamics of the thermal microsystem. The linear PI controller is tuned for the operating region of 55 ^{o}C. As a result, it shows acceptable performance for the corresponding region. But, it shows poor control performances for the other operating points of 72 ^{o}C and 95 ^{o}C because the linear controller cannot remove the nonlinear dynamics.

4.5 PCR Test

Figure 13 shows a fluorescent image of the amplified DNA after PCR in the chip of the developed thermal microsystem and the bulk e-tube of the conventional PCR machine.
DNA was successfully amplified with our microsystem while it took much less time than the conventional machine.

6. CONCLUSIONS

We developed a thermal microsystem composed of a silicon-based microreactor and other equipment/software required for full automation. The dynamic characteristic of the thermal microsystem was analyzed and on the basis of the analysis, the model structure was determined. We identified the model parameters using the prediction error identification method and demonstrated its excellent model performances. A nonlinear control strategy was proposed to linearize the nonlinear dynamics of the thermal microsystem, which makes the tuning of the PI controller easier and guarantees high performances as in the linear case. We could demonstrate a high-performance operation with the anti-windup nonlinear PI controller tuned by the optimal tuning method. The PCR of plasmid DNA was performed successfully with the developed microsystem.

ACKNOWLEDGMENT

This work is supported by the BK21 Project and Center for Ultramicrochemical Process Systems sponsored by KOSEF.

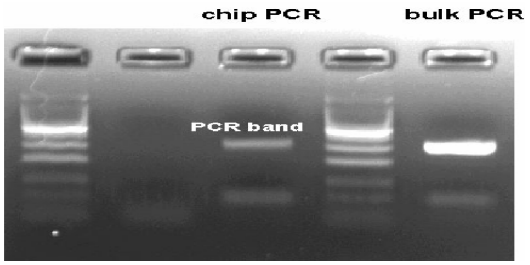

Figure 13. Slab gel electrophoresis for PCRs of the thermal microsystem and the conventional machine.

REFERENCES

Belgrader P., Young S., Yuan B., Primeau M., Christel L. A., Pourahmadi F. and Northrup M. A. (2001), A Battery-Powered Notebook Thermal Cycler for Rapid Multiplex Real-Time PCR Analysis, *Anal. Chem.*, **73**, 286-289

Lao A.I.K., Lee T.M.H., Hsing I. and Ip N. Y. (2000), Precise Temperature Control of Microfluidic Chamber for Gas and Liquid Phase Reactions, *Sens. Actuators*, **84**, 11-17

Morari, M. and Zafiriou, E. (1989), *Robust Process Control*, Prentice-Hall, Englewood Cliffs, NJ

Northrup M. A., Benett B., Hadley D., Landre P., Lehew S., Richards J. and Stratton P. (1998), A Miniature Analytical Instrument for Nucleic Acids Based on Micromachined Silicon Reaction Chambers, *Anal. Chem.*, **70**, 918-922

Seborg, D.E., Edgar, T. F. and Mellichamp, D. A. (1989), *Process Dynamics and Control*, John Wiley & Sons, Inc.

Sung, S.W. and Lee, I. (2001), Prediction Error Method for Continuous-time Processes with Time Delay, *Ind. Eng. Chem. Res.*, **40**, 5743-5751

Sung S. W., Lee T. and Park S. (2002), Optimal PID Controller Tuning Method for Single-Input-Single-Output (SISO) Processes, *AIChE J.*, **48**,1358-1361